

1 **Variations of atmospheric PAHs concentrations, sources, health risk, and direct**
2 **medical costs of lung cancer around the Bohai Sea under the background of**
3 **pollution prevention and control in China**

4

5 Wenwen Ma^{1,4,5}, Rong Sun^{1,4,*}, Xiaoping Wang³, Zheng Zong^{1,4}, Shizhen Zhao², Zeyu Sun^{1,4,5},
6 Chongguo Tian^{1,4,*}, Jianhui Tang^{1,4}, Song Cui⁶, Jun Li², Gan Zhang²

7

8 ¹ CAS Key Laboratory of Coastal Environmental Processes and Ecological Remediation, Yantai
9 Institute of Coastal Zone Research, Chinese Academy of Sciences, Yantai Shandong 264003, P.R.
10 China

11 ² State Key Laboratory of Organic Geochemistry, Guangzhou Institute of Geochemistry, Chinese
12 Academy of Sciences, Guangzhou, 510640, China

13 ³ Ludong University, Yantai, 264025, China

14 ⁴ Shandong Key Laboratory of Coastal Environmental Processes, Yantai Shandong 264003, P.R.
15 China

16 ⁵ University of Chinese Academy of Sciences, Beijing, 100049, China

17 ⁶ International Joint Research Center for Persistent Toxic Substances (IJRC-PTS), School of Water
18 Conservancy and Civil Engineering, Northeast Agricultural University, Harbin 150030, China

19

20 * Correspondence to: Rong Sun (rsun@yic.ac.cn) and Chongguo Tian (cgtian@yic.ac.cn)

21

22 **Abstract.** The Bohai Sea (BS) as one of the severe polluted areas of polycyclic aromatic hydrocar-
23 bons (PAHs) in China has been received wide attention in recent decades. To characterize the var-
24 iations of concentrations and sources of PAHs from June 2014 to May 2019, fifteen congeners of
25 PAHs ($\sum_{15}\text{PAHs}$) were measured from atmospheric samples (N=228) collected at 12 sites around
26 the BS, and health risk and direct medical costs associated with lung cancer exposed to PAHs were
27 also estimated. The annual daily average concentration of $\sum_{15}\text{PAHs}$ was $56.78 \pm 4.75 \text{ ng m}^{-3}$, dom-
28 inated by low molecular weight (LMW-PAHs, 3-ring) ($58.7 \pm 7.8\%$). During the five-year sampling
29 period, the atmospheric $\sum_{15}\text{PAHs}$ concentration reduced by 17.5% for the whole BS, especially in
30 the tightly controlled area of Tianjin (TJ) with a drop of 51.7%, which was mainly due to the de-
31 crease of high molecular weight PAHs (HMW-PAHs, 5-6 ring) concentration. Generally, the con-
32 centration of $\sum_{15}\text{PAHs}$ was the highest in winter and the lowest in summer, mainly attributed to the
33 change of LMW-PAHs concentration. Based on PMF model, PAHs at the BS were mainly ascribed
34 to coal combustion and biomass burning. And the contribution of coal combustion and motor ve-
35 hicle to PAHs had a different performance between the BS (coal combustion rose by 7.2%, motor
36 vehicle fell by 22.4%) and TJ (coal combustion fell by 12.6%, motor vehicle rose by 6.9%). The
37 incidence of lung cancer (ILCR) caused by exposing to atmospheric PAHs at the BS and TJ de-
38 creased by 74.1% and 91.6% from 2014 to 2018, respectively. That was mainly due to the decrease
39 of the concentration of highly toxic HMW-PAHs. It was reflected on the savings of \$10.7 million
40 in direct medical costs of lung cancer exposed PAHs, which was accounted 46.1% before air pre-
41 vention and control around the BS. And there was a higher cost reduction of 54.5% in TJ. Hence,
42 this study proved that implementing pollution prevention and control not only effectively reduced
43 the concentration of pollutants and the caused risks, but also significantly reduced the medical costs
44 of diseases caused by corresponding expose.

45

46 **1 Introduction**

47 Polycyclic aromatic hydrocarbons (PAHs) were a class of classical organic compounds with
48 at least two benzene rings, and have been received long-term attention because of cytotoxic, tera-
49 togenic, mutagenic, or carcinogenic (Colvin et al., 2020; Marvin et al., 2020). The United States
50 Environmental Protection Agency (USEPA) identified sixteen PAH congeners as priority pollutants
51 (Lv et al., 2020). Previous studies were shown that PAHs in the atmosphere of heavily polluted
52 areas such as factories and the urban posed a threat to human health, especially the respiratory
53 system (Agudelo-Castañeda et al., 2017; Ramírez et al., 2011). Because of their relatively high
54 concentration, strong toxic potency, and long-term distance transmission, the PAHs congeners in
55 the atmosphere were considered as a major factor of lung cancer risk to the public (Ma et al., 2010;
56 Gong et al., 2011; Ma et al., 2013; Hong et al., 2016). According to the statistics, the incidence and
57 mortality of lung cancer were ranked first among cancer-related cases in the world, and so the lung
58 cancer risk owing to exposing to PAHs was of particular concern and widely assessed (Křůmal and
59 Mikuška, 2020; Liao et al., 2011; Taghvaei et al., 2018; Zhang et al., 2023).

60 PAHs were emitted primarily via incomplete combustion and pyrolysis of carbon-contained
61 materials, such as fossil fuels and biomass (Biache et al., 2014). China has been assessed as the
62 largest emitter of PAHs all over the world for recent two decade because of rapid development of
63 the economy and increasing consumption of carbon-contained materials (Zhang et al., 2007), par-
64 ticularly at the Bohai economic zone, as the third developing economic pole. (Sun et al., 2022).
65 PAHs pollution in the atmosphere of the Bohai Sea (BS) was in a severe situation (Wang et al.,
66 2018). The Bohai economic zone included the Beijing-Tianjin-Hebei (BTH) region, the Liaodong
67 Peninsula, and the Shandong Peninsula. The BTH region was the center of economic development
68 of the Bohai Rim economic area. (Liang et al., 2018; Zhang et al., 2016) Hence, the Beijing-Tianjin-
69 Hebei (BTH) region was one of the regions with the highest PAHs emission intensity and the heav-
70 iest atmospheric PAHs concentrations in China (Zhang et al., 2007; Zhang et al., 2016). In such
71 serious pollution, the health risk exposed to PAHs caused great concern. The population attributable
72 fraction (PAF) for lung cancer caused by inhalation of PAHs in the atmosphere of the BTH area

73 was more than twice higher than the mean value in whole China in 2009 (Zhang et al., 2009). The
74 incremental lifetime cancer risk (ILCR) of the PAHs exposure at Tianjin was in the range of $1 \times$
75 10^{-5} to 1×10^{-3} in 2008, which was much higher than the mean level of 4.56×10^{-6} in China (Lian
76 et al., 2021; Bai et al., 2009). The annual lung cancer morbidity of Tianjin (6.99×10^{-6}) within the
77 BTH region was the highest city among 35 cancer registries in China (Zhang et al., 2007). Mean-
78 while, with the frequent occurrence of haze in the BTH region, more attention has been paid to
79 concentration levels and health risk of fine particulate matter with aerodynamic equivalent diameter
80 $\leq 2.5 \mu\text{m}$ ($\text{PM}_{2.5}$) since 2013 (Chen et al., 2020).

81 $\text{PM}_{2.5}$ pollution in China has obviously been improved since the Air Pollution Prevention and
82 Control Action Plan (2013-2017) and the Three-year Action Plan for Winning the Blue-Sky De-
83 fense Battle (2018-2020) were proposed by the Chinese government in 2013 and 2018 (Zhao et al.,
84 2023). As one of the severely polluted areas in China, the improvement was more significantly at
85 the BTH region, which implemented the strictest pollution control policy (Li et al., 2020). As re-
86 ported that the concentration of $\text{PM}_{2.5}$ at the BTH region dropped by 52% from $106 \mu\text{g m}^{-3}$ in 2013
87 to $51 \mu\text{g m}^{-3}$ in 2020 (Bulletin of the State of China's ecological Environment, 2021). In the pre-
88 vention and control of pollution policies, reducing emissions of coal combustion and motor vehicle
89 were the major parts (Guo et al., 2018; Li et al., 2019). The two sources have been recognized as
90 primary contributors to PAHs in the atmosphere as well (Lin et al., 2015; Han et al., 2018). As a
91 result, the controls of the two sources not only reduced $\text{PM}_{2.5}$ emission, but also PAHs emission
92 (Zhi et al., 2017). During the controlling processes, the variations in the concentrations and health
93 risk of $\text{PM}_{2.5}$ at BTH region have been well identified (Fang et al., 2016; Yan et al., 2019), while
94 the relevant understanding of PAHs in the region urgently needs to be updated. Especially, the
95 statistical data of the lung cancer risk due to exposing to PAHs was established ten years ago (Zhang
96 et al., 2009; Lian et al., 2021).

97 To track changes in concentrations and source of atmospheric PAHs and estimate health risk
98 and the direct medical costs associated with lung cancer by exposing to PAHs during the air pollu-
99 tion control actions, a field monitoring campaign was conducted at twelve sites around the BS for

100 five years from June 2014 to May 2019. The measures for air pollution control implemented were
101 different at the BTH region, the Liaodong Peninsula, and the Shandong Peninsula (Huang et al.,
102 2017). Thus, it would provide us an opportunity to understand the difference in environmental
103 concentrations, source contributions, and health risk of PAHs. The main aims of this study were (1)
104 to characterize the spatial and temporal changes of the concentrations and components of PAHs in
105 the atmosphere around the BS, (2) to evaluate the difference of source contributions of PAHs, and
106 (3) to assess the changes of direct medical costs for treating lung cancer caused by inhalation ex-
107 posure to PAHs under atmospheric prevention and control in the five years.

108 **2 Materials and methods**

109 **2.1 Sampling site and sample collection**

110 The sampling sites for this study had been reported in previous literatures (Sun et al., 2021),
111 and it was briefly introduced here. The information of the sites was shown in Table S1 of the Sup-
112 porting Information (SI). Twelve air sampling sites were located at Beihuangcheng (BH), Dalian
113 (DL), Donggang (DG), Dongying (DY), Gaizhou (GZ), Longkou (LK), Laoting (LT), Rongcheng
114 (RC), Tianjin (TJ), Xingcheng (XC), Yantai (YT), and Zhuanghe (ZH). A passive air sampler with
115 polyurethane foam (PUF, 14.00 cm diameter \times 1.35 cm thickness) was used to collect atmospheric
116 samples at each sampling site (Eng et al., 2014). The PUF disks were deployed around 1.5–2.0 m
117 above the ground, the sampling duration was about 3 months for one batch. 228 samples were
118 collected from June 2014 to May 2019. The sampling rate of atmospheric PAHs was $3.5 \text{ m}^3 \text{ day}^{-1}$
119 (Jaward et al., 2005; Moeckel et al., 2009). Prior to sampling, the PUF disks were pre-cleaned by
120 methanol, acetone, and hexane, respectively. The extracted PUF disks were placed in airtight con-
121 tainers and stored at $-18 \text{ }^\circ\text{C}$ before the sampling campaign. After sampling, the samples were pre-
122 pared and then stored at a $-18 \text{ }^\circ\text{C}$ freezer in the lab for further analyses.

123 **2.2 Sample pretreatment and instrumental analysis**

124 The five PAHs surrogates (Naphthalene- D_8 , Acenaphthene- D_{10} , Phenanthrene- D_{10} , Chrysene-
125 D_{12} , Perylene- D_{12}) and the activated copper fragments were added in advance (Qu et al., 2022).
126 The samples were extracted for 24 h, which the elution was acetone and hexane (200mL, v:v=1:1)

127 through Soxhlet apparatus. The extracted solution was concentrated to 1mL with rotary evaporator
128 (SHB-III, Zhengzhou Greatwall Ltd., China). Then, silica-alumina column was used to obtain the
129 aromatic components, then the targets were obtained with 40 mL of a mixed solution of dichloro-
130 methane and hexane (v:v=1:1). Finally, the eluent was concentrated and reduced to 500 μ L by a
131 gentle nitrogen stream. As the internal standard substance, 400 ng of hexamethylbenzene (Supelco,
132 USA) was added to each sample solution before the instrumental analysis.

133 The targets were detected through the gas chromatograph equipped with mass spectrometry
134 (GC-MS, Agilent 5975C-7890A, USA), and the chromatographic column was DB-5MS (Agilent
135 Technologies, 30 m \times 0.25 mm \times 0.25 μ m). Each extract was injected by 1 μ L with splitless mode.
136 High-purity helium (purity \geq 99.99%) with a flow rate of 1.3 mL min⁻¹ was used as the carrier gas.
137 The process of oven temperature was set as at 80 °C with a hold of 3 minutes, and then raised to
138 310 °C by 10 °C min⁻¹, and then hold 10 minutes. The temperatures of inlet and ion source were
139 290 °C and 230 °C, respectively. The details of the targeted compounds were shown in Table S2 of
140 SI. Seven gradients of mixed solutions were established for quantitative calculation of PAHs. More
141 details were reported in previous study (Wang et al., 2018).

142 **2.3 Quality assurance and quality control**

143 The mean recovery values of Naphthalene-D₈, Acenaphthene-D₁₀, Phenanthrene-D₁₀, Chrysene-
144 D₁₂, and Perylene-D₁₂ were 77.3%, 85.9%, 87.5%, 88.3%, and 92.8%, respectively, which were
145 ranging from 66.5% to 123.1%. All the relative deviations were within 20%, except for Naphtha-
146 lene-D₈. Nap was excluded because of its low recovery, and the other fifteen PAHs (Σ_{15} PAHs) were
147 used for further discussion in this study. For each batch of twelve PUF samples, a field blank and
148 a procedural blank were also analyzed at same treatment process. In this study, the method detection
149 Limits (MDLs, defined as the mean blank value plus 3 times the standard deviation) for 15 PAH
150 congeners ranged from 0.02 to 0.13 ng sample⁻¹, which were shown in Table S2 of SI. The final
151 concentrations were not surrogate-corrected. The glassware was all cleaned and burned for 8 hours
152 in muffle oven at 450 °C before the experiment. The solvents were chromatography-pure or had
153 been redistilled and purified before using.

154 2.4 Source apportionment of PAHs

155 The model of positive matrix factorization (PMF) released by the USEPA (PMF 5.0) was used
156 to apportion the emission sources of PAHs in this study. The basic calculation formula of the PMF
157 method is as Eq. (1):

$$158 \quad x_{ij} = \sum_{k=1}^p g_{ik} f_{kj} + e_{ij} \quad (1)$$

159 where p represents the number of sources identified by the PMF model. x_{ij} represents original
160 concentration data of i^{th} chemical species and j^{th} sample. f_{ik} represents the source profile of k^{th}
161 source and j^{th} chemical species. g_{kj} represents contribution ratio of k^{th} source to j^{th} sample. e_{ij} rep-
162 represents the simulated residual error of i^{th} chemical species and j^{th} sample. Source contributions and
163 profiles are solved by the PMF model minimizing the objective function Q , as Eq. (2):

$$164 \quad Q_{\min} = \sum_{i=1}^n \sum_{j=1}^m \left(\frac{x_{ij} - \sum_{k=1}^p g_{ik} f_{kj}}{u_{ij}} \right)^2 \quad (2)$$

165 where x_{ij} , g_{ik} , and f_{kj} are same that in Eq. (1), respectively. u_{ij} is the uncertainty of x_{ij} , and the
166 calculation method of uncertainty is showed in Text S2 of SI. More details have been documented
167 (Sofowote et al., 2011; Paatero et al., 2014).

168 Before the source apportionment, principal component analysis (PCA) was applied to pre-
169 estimate the minimum number of emission sources in this study because PCA was able to explain
170 the overall variables with fewer variables with a minimum loss of information (Liu et al., 2021).
171 SPSS Statistics 25.0 was used to perform the PCA analysis in this study.

172 2.5 Health risk assessment

173 The total toxicity equivalent (TEQ , ng m^{-3}) of the fifteen PAHs with BaP as reference is cal-
174 culated as Eq. (3):

$$175 \quad TEQ = \sum_{i=1}^n (C_i \times TEF_i) \quad (3)$$

176 where C_i is concentration of the i^{th} PAH compound (ng m^{-3}), TEF_i is the cancer potency of the
177 i^{th} PAH compound (dimensionless), as shown in Table S2 of SI.

178 $ILCR$ in this study referred to cancer risk in a population due to exposure to a specific carcin-
179 ogen (Zhuo et al., 2017). Its calculation formula is as Eq. (4):

$$180 \quad ILCR = UR_{BaP} \times TEQ \quad (4)$$

181 In above, UR_{BaP} represents the cancer risk when the concentration of BaP is 1 ng m^{-3} (ng m^{-3})
182 3 . According to the regulations of World Health Organization (WHO), UR_{BaP} can be 8.7×10^{-5} per
183 ng m^{-3} . That is, in terms of life span of 70 years, lifetime exposure to BaP concentration of 1 ng m^{-3}
184 3 resulted in a risk of cancer by inhalation of 8.7×10^{-5} (Luo et al., 2021).

185 **2.6 Medical costs assessment**

186 In this study, the medical costs were assessed by comparing total direct medical costs for
187 treating lung cancer caused by respiratory exposed to PAHs in the atmosphere under the assumption
188 that no air pollution control and the actual implementation of air pollution control. The total direct
189 medical costs for treating lung cancer (C_t) are calculated as Eq. (5):

$$190 \quad C_t = C_{pc} \times P \times I_{add} \quad (5)$$

191 where C_t is the total direct medical costs of lung cancer induced by PAHs exposure, C_{pc} is the
192 per capita direct medical costs of lung cancer, and a cost of \$8,700 in China in 2014 was used in
193 this study (Shi et al., 2017). P is the annual population, I_{add} is the additional incidence of lung cancer
194 due to PAHs inhalation exposure, it is calculated as Eq. (6):

$$195 \quad I_{add} = I \times PAF \quad (6)$$

196 where I is the incidence of lung cancer. And the I value was 87.37×10^{-5} at Tianjin estimated
197 in 2012, which was referred in this study (Cao et al., 2016). PAF is the population attributable
198 fraction, defined as the decrease in the incidence or mortality of a disease when a certain risk factor
199 is completely removed or reduced to another lower reference level (Menzler et al., 2008). The PAF
200 can be calculated as Eq. (7):

$$PAF = \frac{rr(TEQ) - 1}{rr(TEQ)} \quad \text{and} \quad rr(TEQ) = [URR_{cum, exp = 100}]^{(TEQ \times 70 / 100)} \quad (7)$$

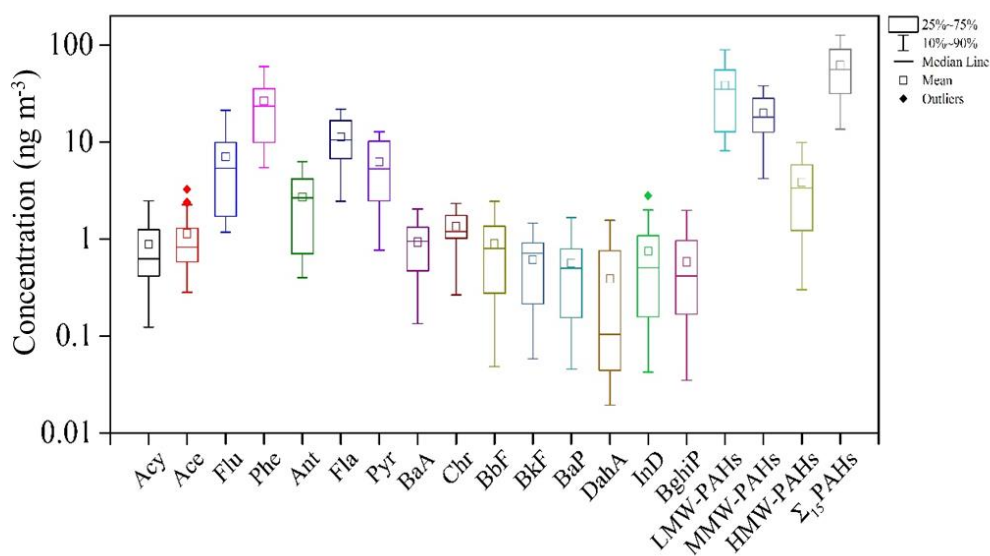
where *rr* is relative risk, that is, the risk of exposure to a specific concentration relative to no exposure. *URR* is the unit relative risk, a reference value of 4.49 per 100 $\mu\text{g m}^{-3}$ years of *BaP* exposure was adopted in this study (Zhang et al., 2009). This reference value was based on an epidemiological study on lung cancer conducted in Xuanwei, China (Menzler et al., 2008) (Gibbs et al., 1997). This study assumed that the mean life expectancy in China was 70 years, and the lifetime exposure was equivalent to 70 years.

3 Results and discussions

3.1 Concentration and composition of PAHs

3.1.1 General information of PAHs

Figure 1 summarizes the annual daily average concentrations of 15 PAHs in the atmosphere at the twelve sampling sites around the BS from June 2014 to May 2019. The annual daily average concentration of Σ_{15} PAHs around the BS was $56.78 \pm 4.75 \text{ ng m}^{-3}$, with a range of 51.39 – 63.55 ng m^{-3} . And the highest concentration was the low molecular weight PAHs (LMW-PAHs, 3-ring), followed by middle molecular weight PAHs (MMW-PAHs, 4-ring) and high molecular weight PAHs (HMW-PAHs, 5-ring and 6-ring), which were accounting for 58.7%, 34.8%, and 6.7% of the total concentration, respectively. The atmospheric PAHs concentration was dominated by the LMW-PAHs in this study, which Phe, Fla, and Flu were the main compounds accounting for 37.7%, 19.8%, and 12.6% of the total. The atmospheric PAHs concentrations around the BS were at a higher pollution level than the Yangtze River Delta and the Pearl River Delta, such as Ningbo (45 ng m^{-3}) (Tong et al., 2019) and Guangzhou (9.72 ng m^{-3}) (Yu et al., 2016). And the atmospheric concentrations of PAHs around the BS were also much higher than in atmosphere above the Great Lakes (1.3 ng m^{-3}) (Li et al., 2021) and southern Europe cities (3.1 ng m^{-3}) (Alves et al., 2017). Overall, it was found that the pollution of atmospheric PAHs around the BS was still worrying.



226 **Figure 1.** Atmospheric concentrations of polycyclic aromatic hydrocarbons (PAHs) around the BS
 227 from June 2014 to May 2019.

228

229 3.1.2 Temporal variations of PAHs

230 For seeking better understand the variation characteristics of PAHs in the atmosphere, the
 231 summer of the previous year to the spring of the next year were taken as a statistical cycle. The
 232 concentrations of Σ_{15} PAHs in the five annual cycles around the BS were $63.55 \pm 58.43 \text{ ng m}^{-3}$
 233 (2014-2015), $55.50 \pm 37.94 \text{ ng m}^{-3}$ (2015-2016), $60.90 \pm 31.13 \text{ ng m}^{-3}$, (2016-2017), 51.39 ± 29.41
 234 ng m^{-3} (2017-2018), and $52.50 \pm 40.08 \text{ ng m}^{-3}$ (2018-2019), respectively (Table S3 of SI). Overall,
 235 the concentrations of Σ_{15} PAHs from June 2014 to May 2019 showed a slow downward trend with
 236 a decrease of 17.5%. The decrease of atmospheric PAHs concentrations was mainly due to the
 237 decline of the HMW-PAHs concentrations. The HMW-PAHs composition ratio decreased from
 238 11.3% (2014-2015) to 3.4% (2018-2019), while the MMW-PAHs raised from 35.5% (2014-2015)
 239 to 41.2% (2018-2019). The LMW-PAHs composition ratio was stable from 53.4% (2014-2015) to
 240 55.4% (2018-2019). The one factor that effected the concentrations of PAHs in the atmosphere
 241 after they were discharged from the emission source was meteorological conditions (Fan et al.,

242 2021), and the other important factor was the amount of the direct emission from the emission
243 source (Ma et al., 2018). The sources of PAHs with different ring numbers were different (Li et al.,
244 2021). LMW-PAHs were mainly produced in the combustion process of non-petroleum sources,
245 while HMW-PAHs were mainly from high temperature combustion products generated by fossil
246 fuel combustion, including some activities involving pyrolysis process, such as vehicle emissions,
247 industrial productions, and other high-temperature source emissions (Zhang et al., 2018; Xing et
248 al., 2020). The significant decrease of HMW-PAHs concentrations at the BS during the five-year
249 observation period might be related to the decrease of high temperature emission sources. Due to
250 the high toxicity characteristics of HMW-PAHs (Biache et al., 2014; Ma et al., 2020), the decrease
251 of its concentration might indicate a decrease in the environmental toxicity of PAHs.

252 The seasonal distributions of PAHs concentrations in the atmosphere of the BS region showed
253 high in cold season and low in warm season. The concentrations of Σ_{15} PAHs in four seasons were
254 as follow: winter ($104.32 \pm 9.50 \text{ ng m}^{-3}$) > autumn ($53.94 \pm 9.10 \text{ ng m}^{-3}$) > spring (43.89 ± 19.54
255 ng m^{-3}) > summer ($26.28 \pm 13.42 \text{ ng m}^{-3}$) (Table S5 of SI). The concentration of PAHs in winter
256 was about 4 times higher than that in summer, and the maximum and minimum of the annual daily
257 average concentrations at 12 sampling point mostly occurred in winter and summer. In addition,
258 there were significant differences between total PAHs concentration and different ring number con-
259 centrations ($p < 0.05$, the difference level is shown in Table S6 of SI). The seasonal characteristics
260 of PAHs concentrations in this study were consistent with reported results in North China (Ma et
261 al., 2017; Zhang et al., 2019). Interestingly, it was that the difference of PAHs concentrations in
262 four seasons was mainly on account of LMW-PAHs. This indicated that there were nonnegligible
263 pollution sources for LMW-PAHs, especially in winter at the BS region. Then identifying the
264 source of LMW-PAHs was crucial for improving environmental quality of the BS. Studies have
265 shown that coal burning emissions and biomass burning were the main sources of atmospheric
266 PAHs in this region (Liu et al., 2019). In terms of the per capita fuel consumption spatial distribu-
267 tion, the north and west China were apparently higher than that of southeast China, principally
268 because of the difference in winter heating fuel consumption. Therefore, there were significant

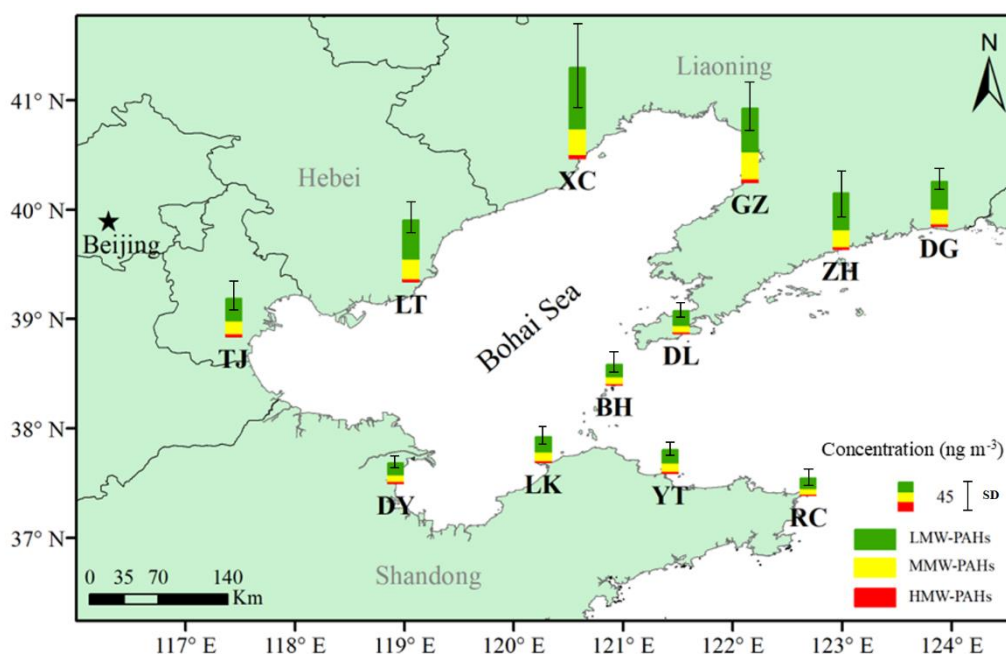
269 seasonal variations of per capita fuel consumption, with peak consumption in the winter months
270 being about twice as high as in the summer months. (Zhu et al., 2013). In addition, due to the
271 migration characteristics of atmospheric PAHs, meteorological conditions such as temperature and
272 wind direction in different seasons would also affect the observed concentration (Tan et al., 2006).
273 And low temperature and inversion layer in winter were not conducive to atmospheric diffusion,
274 resulting in a relatively high concentration of PAHs in the atmosphere near the surface (Wang et
275 al., 2018).

276 **3.1.3 Spatial characteristics of PAHs**

277 Figure 2 and Table S7 of SI displays the distribution of the five-year mean concentrations of Σ_{15}
278 PAHs from June 2014 to May 2019 at the 12 sampling sites around the BS. The concentrations of
279 atmospheric Σ_{15} PAHs ranged from $25.92 \pm 6.41 \text{ ng m}^{-3}$ (RC) to $103.71 \pm 39.11 \text{ ng m}^{-3}$ (XC). The
280 concentrations of PAHs on the BS north coast were twice higher than at the BS south coast. PAHs
281 were a class of pollutants that can undergo long-range transport in the atmosphere (Wang et al.,
282 2018), and their spread was largely affected by local meteorological conditions (Ding et al., 2005).
283 The climate in North China and the adjacent oceanic area was greatly affected by the East Asian
284 monsoon, and the characteristic weather phenomenon in the winter monsoon was the strong north
285 and northwest winds (Tian et al., 2009). Due to the additional emissions from fuel consumption for
286 domestic heating in the source areas, the atmospheric PAHs concentrations significantly increased
287 (Feng et al., 2007; Gao et al., 2016). Combined with backward trajectory shown in Fig. S4 of SI, it
288 suggested that the elevated PAH concentrations in winter at the north of the BS were mainly at-
289 tributed to their outflow from the north and northwest source regions carried by the winter monsoon
290 winds. According to the distribution of atmospheric PAHs in some representative parts of northern
291 China, it was found that the Beijing-Tianjin-Hebei region was greatly affected by nearby sources,
292 while Shandong province and other places were mainly affected by regional emissions. (Zhang et
293 al., 2016) However, the composition of PAHs at the north-south showed consistency without no
294 significant differences (Table S8 of SI). As the whole, the composition of PAHs at 12 station that
295 the highest content was LMW-PAHs (North: 60.0%, South: 57.4%), followed by MMW-PAHs

296 (North: 32.7%, South: 32.4%), and HMW-PAHs was the lowest (North: 7.3%, South: 10.8%). The
297 above indicated that there were the same emission sources of PAHs in the atmosphere around the
298 BS.

299 However, for TJ, the study found that there was a more significant change in the concentration
300 of atmospheric PAHs, which decreased from 68.61 ng m⁻³ (2014-2015) to 33.14 ng m⁻³ (2018-
301 2019). The reason was mainly that TJ was located at the Beijing-Tianjin-Hebei region where was
302 the strictest area of air pollution prevention and control, as a key area in China's "12th Five Year
303 Plan". For exploring the potential differences of source emissions at 12 sampling points, Pearson
304 correlation analysis was used to analyze the seasonal distribution of PAHs concentrations as shown
305 in Table S9 of SI. Among the five stations (LK, DY, TJ, LT, and XC) at the western BS centered on
306 TJ, the correlation coefficients of atmospheric PAHs concentration (0.72–0.89) among the other
307 four stations were greater than that between each site and TJ (0.50–0.68). That the co-variability
308 of PAHs concentrations between TJ and the other four stations was weaker. This indicated that
309 there were certain differences between TJ's PAHs emission sources and adjacent areas.

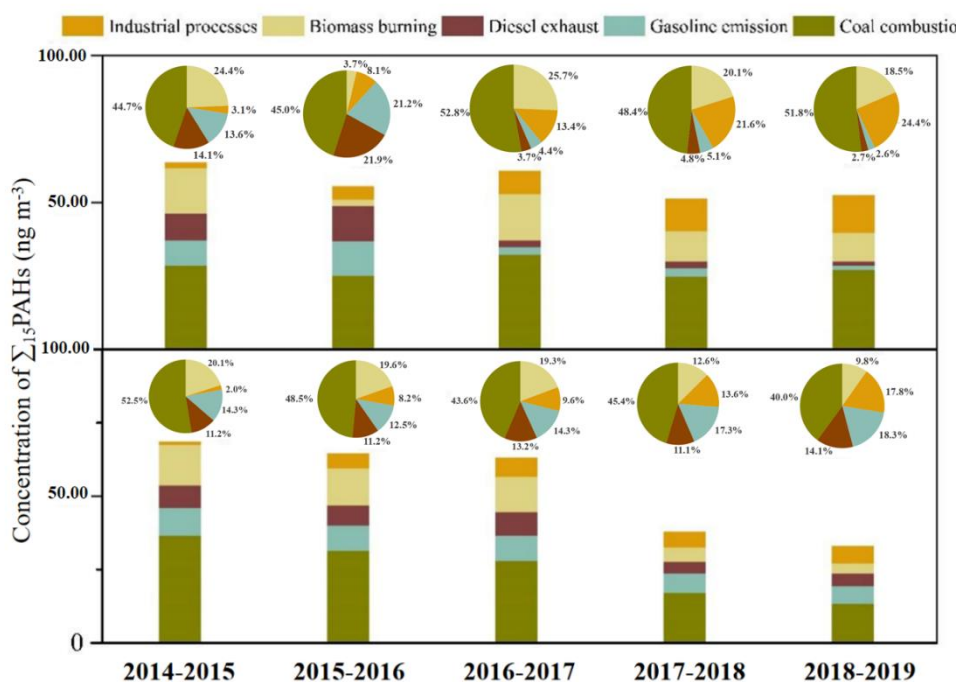


310
311 **Figure 2.** The mean concentration distribution of Σ₁₅ PAHs at 12 sites around the BS from June
312 2014 to May 2019.

313

314 **3.2 Source apportionment of PAHs**

315 For further probing into the causes for the variations of the concentrations and compositions
316 of PAHs, the sources apportionment of PAHs in the atmosphere around the BS and TJ region from
317 2014-2015 to 2018-2019 was investigated via PCA and PMF. PCA analysis results showed that
318 when four factors (eigenvalues > 1) were extracted from the data set, the total cumulative load
319 accounted for more than 85% of the variance (Table S10 of SI). This indicated that at least four
320 types of emission sources could better explain the source of atmospheric PAHs. For PMF model,
321 the key process was to determine the correct number of factors, and this study was based on the
322 results of PCA. Based on the random seed, 4 – 7 factors were used through the PMF model for
323 source analytical simulation. The source analytical simulation of five factors determined the most
324 stable results and the most easily interpreted factors. The solution produces Q values (both robust
325 and true) that were close to the theoretical Q values, which was indicating that the PAHs data set
326 in the modeling input provided appropriate uncertainty (Sun et al., 2021). The data set used for
327 PMF analysis included the concentrations of 228 samples of 15 PAHs and uncertainties. The diag-
328 nostic regression R^2 value for the overall concentrations of 15 PAHs components was 0.986. The
329 predicted concentrations of 15 PAHs via PMF model were almost consistent with the actual con-
330 centrations of 15 PAHs around the BS (Fig. S5–S6 of SI and Text S2 of SI). It meant that the model
331 results were good and could be used as the judgment basis for source analysis of target species, so
332 these 5 factors would well explain the source of PAHs. Contribution of source identified by PCA
333 and PMF were coal combustion, biomass burning, industrial processes, gasoline emission, and die-
334 sel emission. The detailed information of source identification is shown Text S3 of SI.



335

336 **Figure 3.** Concentration and source contribution of Σ_{15} PAHs sources around the BS (the upper
 337 part) and TJ (the lower part) from 2014-2015 to 2018-2019.

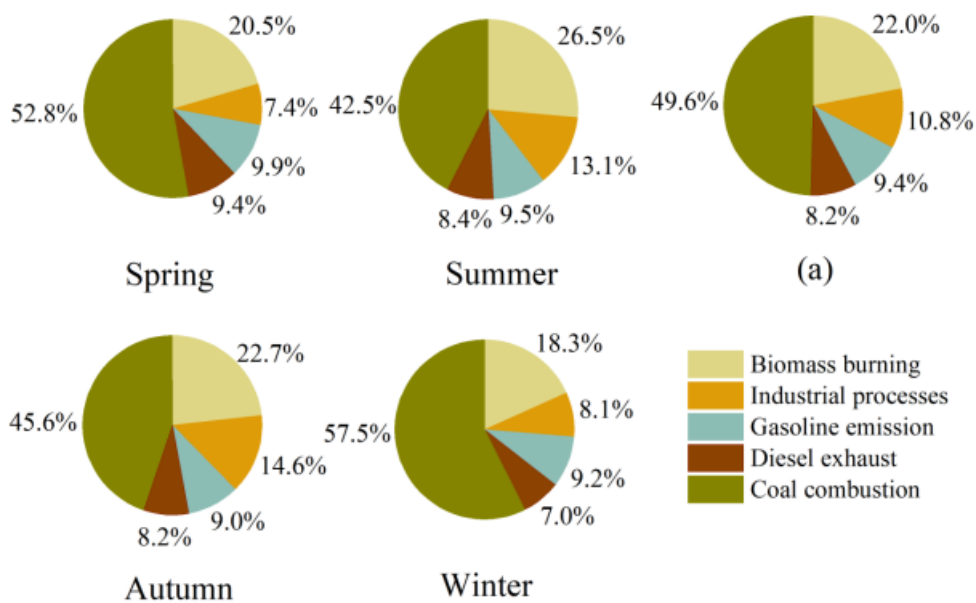
338

339 Fossil fuels combustion emissions were the reason for the significant increase of atmospheric
 340 pollutants, and that were also responsible for the elevated $PM_{2.5}$ levels around the BS region (Yang
 341 et al., 2017). To explore the relationship between Σ_{15} PAHs and $PM_{2.5}$ concentrations, available
 342 online $PM_{2.5}$ data for eight cities that on behalf of sampling sites (DG, DL, DY, GZ, LT, TJ, XC,
 343 and YT) (Air quality historical data query, 2014-2019) were collected, which averaged their con-
 344 centrations according to the sampling periods in the study (Table S12 of SI). The Pearson correla-
 345 tion coefficients of the concentrations of atmospheric PAHs and $PM_{2.5}$ were ranging from 0.485 to
 346 0.868, and the significant levels were greater than 95% as listed in Table S13 of SI. During the
 347 observation of the five-year, the $PM_{2.5}$ concentration at the BS region decreased by 29.6% from 57
 348 $\mu g m^{-3}$ to 40 $\mu g m^{-3}$, and at TJ showed an even greater decrease by 33.8% from 78 $\mu g m^{-3}$ to 51 μg
 349 m^{-3} . From 2013, $PM_{2.5}$ had been strictly controlled by the government year by year, which the
 350 significant correlation indicated that the PAHs concentrations should be affected. To explore the
 351 potential influencing factors of the difference in atmospheric PAHs composition between the BS

352 area and TJ, their average annual contributions of various PAHs emission sources from 2014-2015
353 to 2018-2019 were compared shown in Figure 3. During the sampling period of the BS region, coal
354 combustion was the main source of the atmospheric PAHs emission (44.7%), followed by biomass
355 burning (24.4%) in 2014-2015, which was switching to coal combustion (51.8%) and industrial
356 processes (24.4%) in 2018-2019. For TJ, coal combustion was also the main source of the atmos-
357 pheric PAHs emissions (52.5%), followed by biomass burning (20.1%) in 2014-2015, which was
358 switching to coal combustion (40.0%), industrial processes (17.8%) and gasoline emissions (18.3%)
359 in 2018-2019. The source contributions of coal combustion to atmospheric PAHs had increased by
360 7.2% around the BS, while the corresponding contributions in TJ had fallen by 12.6%. The absolute
361 contribution (the total concentration of PAHs multiplied by the percentage value of the contributing
362 source) decreased, which was indicating that the reduction of the coal contribution source had a
363 significant improvement on the atmospheric PAHs pollution.

364 The main source of atmospheric PAHs around the BS was coal combustion (Liu et al., 2019; Qu
365 et al., 2022), while for TJ, as one of the key areas for air pollution control in China, had taken
366 stricter measures to control emissions of coal combustion (Wu et al., 2015). For instance, the city
367 took the lead in the switching domestic fuel from coal to natural gas and electricity in 2017 to
368 reduce emissions of air pollutants (Zhang et al., 2021). These targeted measures had more force-
369 fully controlled coal-combustion emissions for PAHs in TJ than the other places around the BS
370 region (Guo et al., 2018). Vehicle emission (gasoline and diesel exhaust) to atmospheric PAHs had
371 experienced a sharp drop of 22.4% for the BS area, while for TJ risen by 6.9%. The same trend for
372 vehicle emission was found in the study of Beijing and Tianjin (Zhang et al., 2016; Chao et al.,
373 2019). The decrease was mainly due to the elimination and scrapping of substandard vehicles car-
374 ried out by the Chinese government in 2015. Based on the “China Vehicle Environmental Manage-
375 ment Annual Report”, the car ownership around the BS increased by about 17.5 million, but the
376 emissions of hydrocarbons including PAHs reduced by 95,000 tons from 2014 to 2018 (Fig. S8 of
377 SI). The source apportionment showed that the contribution of vehicle emission to PAHs had a
378 sharp decline since the spring of 2016 (Fig. S9 of SI), with a decreased by 38% (19% for gasoline

379 and 19% for diesel) around the BS (Huang et al., 2017). Although the contribution of vehicle emis-
 380 sions for TJ was increased, the concentrations of PAHs was decreasing. It indicated that these
 381 measures had also controlled vehicle emissions and kept the emissions of PAHs at a low level.
 382 Therefore, targeted control measures could effectively control PM_{2.5} and PAHs pollution in the
 383 atmosphere at the BS and TJ. Moreover, PAHs were a kind of organic compounds produced with
 384 black carbon (BC), and, to some extent, the molecular characteristics of PAHs also provided the
 385 basic data to analysis of the source of BC in the atmosphere of the BS (Fang et al., 2016). At the
 386 same time, the PAHs source analysis results of this study revealed that the composition and source
 387 of atmospheric BC in the BS region have also changed from 2014 to 2019. This problem needs our
 388 attention and confirmation.



389
 390 **Figure 4.** The seasonal and average contributions for five sources of Σ_{15} PAHs derived from PMF;
 391 (a): the five-year average contributions of five sources.

392
 393 Figure 4 shows the seasonal distribution of five sources for atmospheric PAHs at the BS. Gen-
 394 erally, the seasonal distribution of five sources for atmospheric PAHs at TJ was consistent with that
 395 the BS, which was not separately discussed here. The relevant information of TJ was shown as Fig.
 396 S10 of SI. Coal combustion was the main emission source in the four seasons, followed by biomass

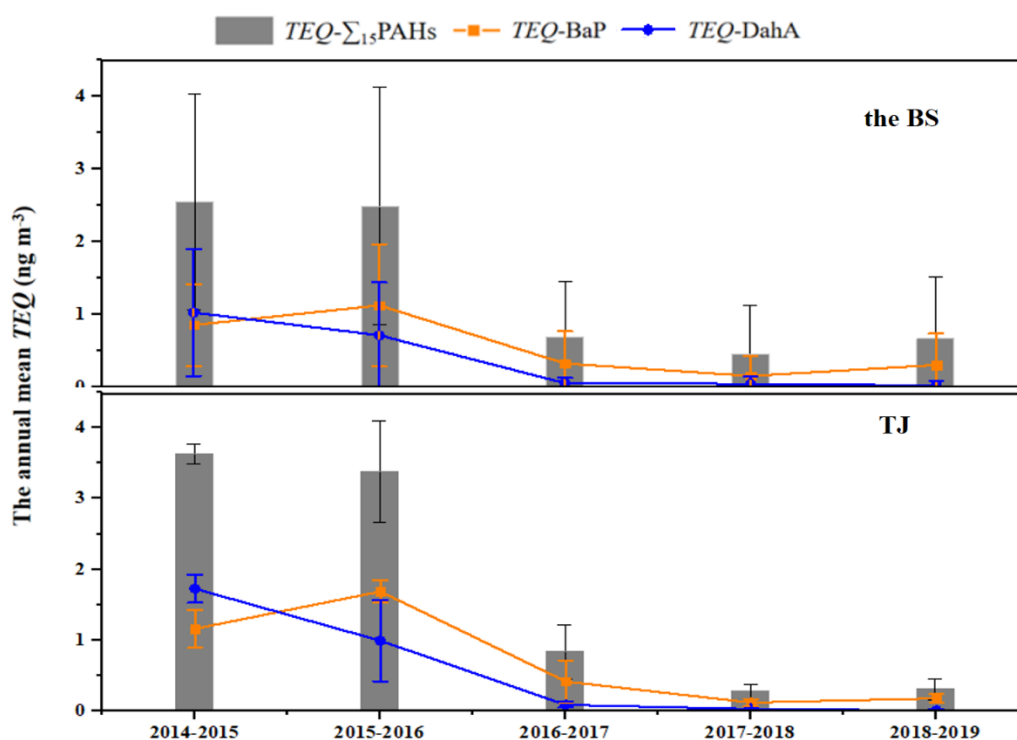
397 burning, while the contributions of the others (industrial processes, gasoline emission, and diesel
398 emission) were similar. Compared with other seasons, the contribution of coal combustion for at-
399 mospheric PAHs to the BS was the highest in winter, which was followed by spring, and the lowest
400 was in summer. This was consistent with the seasonal distributions of the concentrations of PAHs
401 in the atmosphere at the BS. Based on the seasonal distribution of concentrations, the increase
402 concentrations of atmospheric PAHs in winter were mainly caused by coal combustion. This might
403 be due to people in cold winters at northern China rely on coal combustion for heating. For biomass
404 combustion, it was higher in summer and autumn, which was related to straw burning after harvest.
405 Given all this, the seasonal distributions of PAHs sources indicated that the pollution of atmos-
406 pheric PAHs was mainly influenced by human activities.

407 **3.3 Health risk exposed to PAHs**

408 On the basis of the Eq. (3), the annual mean *TEQ* value around the BS was $1.37 \pm 1.05 \text{ ng m}^{-3}$
409 ³ from June 2014 to May 2019, which below the national standard (10 ng m^{-3}) while slightly higher
410 than the WHO standard (1 ng m^{-3}). The HMW-PAHs contributed dominantly 76.4% of the total
411 *TEQ*. However, the concentration of HMW-PAHs in the atmosphere accounted for 6.5% of the total
412 PAH concentration. Among which, the two major *TEQ* contributors were BaP ($38.2\% \pm 8.0\%$) and
413 DahA ($16.6\% \pm 9.0\%$). For TJ, the annual mean *TEQ* value was $1.69 \pm 1.50 \text{ ng m}^{-3}$, which was
414 slightly higher than that the BS. It was indicating that higher health risk was caused by PAHs ex-
415 posed at TJ than around the BS. The HMW-PAHs contributed dominantly 90.9% of the total *TEQ*.
416 However, the concentration of HMW-PAHs in the atmosphere accounted for 8% of total PAHs
417 concentrations. Among which, the two major contributors were BaP ($47.2\% \pm 9.2\%$) and DahA
418 ($19.7\% \pm 16.2\%$).

419 The information of *TEQ* at BS and TJ from June 2014 to May 2019 was shown in Figure 5.
420 The average value of *TEQ* at the BS in the five cycle years was $2.55 \pm 1.49 \text{ ng m}^{-3}$, $2.49 \pm 1.63 \text{ ng}$
421 m^{-3} , $0.69 \pm 0.76 \text{ ng m}^{-3}$, $0.47 \pm 0.66 \text{ ng m}^{-3}$, and $0.67 \pm 0.84 \text{ ng m}^{-3}$, respectively. The value of *TEQ*
422 at the BS showed a downward trend year by year. The environmental health risk of PAHs in the
423 fifth year was decreased by three times than in the first year. It was found that the decrease of

424 HMW-PAHs concentration was the main reason for the decrease of the toxicity of PAHs. For ex-
 425 ample, the concentration of BaP in the atmosphere at the BS decreased by 79.1% in five years, and
 426 the concentration of DahA, as a species with carcinogenic toxicity equivalent to BaP, decreased by
 427 96.1%. For TJ, the average value of *TEQ* in the five cycle years was $3.63 \pm 0.14 \text{ ng m}^{-3}$, $3.38 \pm$
 428 0.72 ng m^{-3} , $0.84 \pm 0.38 \text{ ng m}^{-3}$, $0.28 \pm 0.10 \text{ ng m}^{-3}$, and $0.31 \pm 0.15 \text{ ng m}^{-3}$, respectively. The *TEQ*
 429 value of PAHs in the atmosphere decreased by 91.5% at TJ in the past five years. At TJ, BaP and
 430 DahA as the major contributing factors of *TEQ* in the atmosphere also showed more significant
 431 decline than around the BS. To sum up, the results showed that pollution control could not only
 432 reduce the total concentration of PAHs in the atmosphere at the BS, but also affected the composi-
 433 tion of the PAHs. And it mainly affected the concentration of HMW-PAHs compounds, which the
 434 total toxic equivalent of PAHs in the atmosphere at the BS was remarkably reduced.



435
 436 **Figure 5.** The annual mean *TEQ* of 15 PAHs, BaP, and DahA in the atmosphere at the BS (the
 437 upper part) and TJ (the lower part) from June 2014 to May 2019.

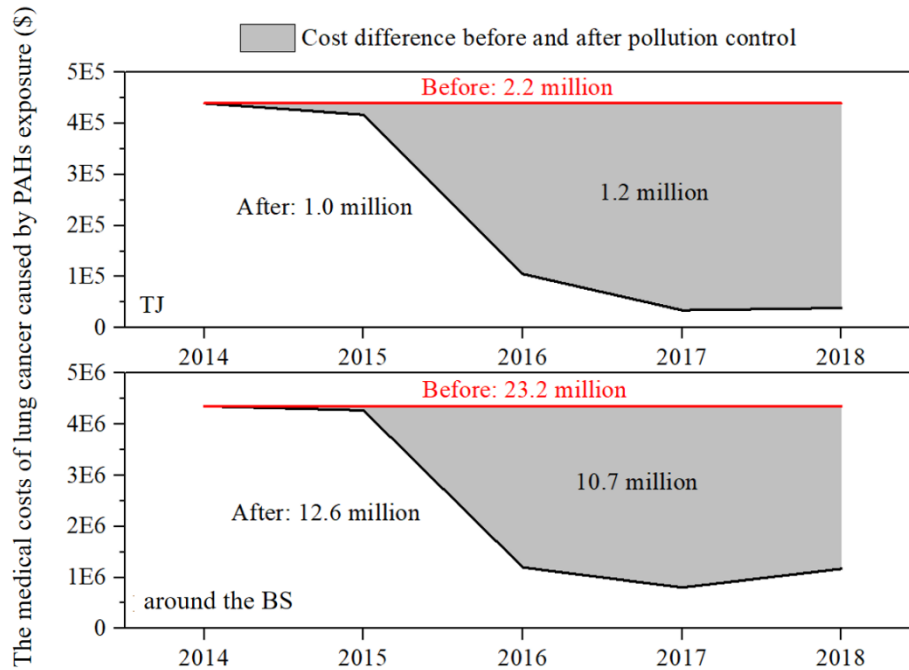
438

439 Simultaneously, incremental lifetime cancer risk (*ILCR*) was used to assess the potential car-
440 cinogenic risk of PAHs in the atmosphere at the BS. According to the USEPA, the *ILCR* value less
441 than 1×10^{-6} was an acceptable risk level. When the *ILCR* value was equal to or high than 1×10^{-6}
442 but less than 1×10^{-4} , which was in a serious risk of cancer, and health issues should be taken
443 seriously. When the *ILCR* value were equal to or greater than 1×10^{-4} , it was considered life-
444 threatening for human. The specific calculation was seen Eq. (4). It was found that the range of
445 *ILCR* value of atmospheric PAHs at the BS region for five years was 4.1×10^{-5} – 2.2×10^{-4} , with an
446 average value of 1.2×10^{-4} , which means that the risk of cancer in this region was in a serious state,
447 and health problems should be paid more attention to. Similarly, to the above *TEQ*, *ILCR* values
448 were also dominated by HMW-PAHs. The *ILCR* caused by PAHs is listed in Table S14 of SI. The
449 *ILCR* at the BS decreased significantly by 74.1% from 2.2×10^{-4} in the first year to 5.7×10^{-5} in
450 the fifth year. Compared with the BS, the *ILCR* at TJ decreased more significantly, from 3.2×10^{-4}
451 to 2.7×10^{-5} by 91.6%. As shown in Table S15 of SI, the study found that the concentration
452 variations of highly toxic BaP and DahA were basically synchronized with the changes of *ILCR*,
453 which implied that the decrease of concentrations of both was the main reason for the cancer risk
454 reduction. The significant reduction of cancer risk at the BS region indicated that the emission of
455 highly toxic HMW-PAHs in the atmosphere has been effectively controlled, which also reflected
456 that the prevention and control of air pollution had effectively reduced the health risk. In particular,
457 the reduction effect of PAHs exposure risk was more obvious at TJ, which air pollution control was
458 strict.

459 **3.4. Direct medical costs of lung cancer caused by exposed to PAHs**

460 This reduction of PAHs health risk would lead to a reduction in the number of people who
461 develop cancer, thus saving on the cost of cancer treatment. In this study, the direct medical costs
462 of lung cancer caused by respiratory exposure to PAHs was estimated by the additional incidence
463 of lung cancer caused by PAHs exposure, the population in the study area, and the direct medical
464 costs per capita of lung cancer patients. The specific calculation was seen Eq. (5). In addition to
465 PAHs exposure, there were many environmental risk factors that could induce lung cancer. For

466 deriving the lung cancer burden caused by atmospheric PAHs respiratory exposure from the inci-
467 dence of lung cancer, this study was characterized by percentage of population risk attribution
468 (*PAF*). The details were seen Eq. (6) and Eq. (7). *PAF* here represented the percentage of reduction
469 in lung cancer incidence which PAHs, an environmental factor, were completely removed or their
470 concentration was reduced. According to the above introduction of *PAF* and analysis of *TEQ*, the
471 directly calculated *PAF* within five years around the BS ranged from 0.5‰ to 2.7‰, with an aver-
472 age value of 1.4‰. The five-year *PAF* at TJ ranged from 0.3‰ to 3.8‰, with an average value of
473 1.7‰. A remarkable situation was that *PAF* around the BS region and TJ decreased significantly in
474 the past five years, from 3.8‰ and 2.7‰ in the first year to 0.3‰ and 0.7‰ in the fifth year re-
475 spectively. The additional lung cancer incidence (*I_{add}*) due to respiratory exposure to PAHs was
476 calculated using the product of lung cancer incidence and *PAF*. Previous studies reported that the
477 incidence of lung cancer at TJ in 2012 was 87.37×10^{-5} (Cao et al., 2016). In this study, $87.37 \times$
478 10^{-5} was used as the reference value of lung cancer incidence. The average *I_{add}* caused by respira-
479 tory exposure to PAHs around the BS region and TJ were 1.26×10^{-6} and 1.55×10^{-6} , respectively.
480 During the observation of the five-year, the *I_{add}* around the BS region and TJ decreased from 2.34
481 $\times 10^{-6}$ and 3.33×10^{-6} in the first year to 6.15×10^{-7} and 2.87×10^{-7} in the fifth year, respectively.
482 The population numbers in the study area were all referred from the public data of the statistical
483 yearbook. The estimated results of the BS region and TJ are shown in Table S16–S17 of SI, respec-
484 tively. It had been reported that the direct cost of an average case of lung cancer patients in China
485 in 2014 was \$9042.79 (Shi et al., 2017; Huang et al., 2016). Since there was no reference data
486 available for other corresponding years, this study took the direct cost per case of lung cancer pa-
487 tients as the baseline in 2014, and the estimate assumed the same direct medical costs per capita
488 for lung cancer within five years.



490 **Figure 6.** The medical costs of lung cancer caused by PAHs exposure before and after the control
 491 of air pollution at TJ and around the BS from 2014 to 2018.

492

493 Figure 6 shows the comparative results of direct medical costs of lung cancer at the BS region
 494 and TJ from 2014 to 2018 under before and after pollution control. In the five years, under the
 495 implementation of air pollution control, the total direct medical costs of lung cancer caused by
 496 respiratory exposure to PAHs in the Bohai Rim region was \$12.6 million. Assuming that no air
 497 pollution control was implemented, the total direct medical costs of lung cancer caused by PAHs
 498 exposure did not change in five years, and the total direct medical costs was \$23.2 million. The
 499 actual implementation of control on the total direct medical costs of lung cancer saved \$10.7 mil-
 500 lion. At TJ, the total direct medical costs of lung cancer induced by respiratory exposure to PAHs
 501 under actual air pollution control was \$1.0 million. Under the assumption that no air pollution
 502 control was implemented, the total direct medical costs of lung cancer caused by PAHs exposure
 503 was \$2.2 million, saving about \$1.2 million at TJ. Compared to without air pollution control, the
 504 total direct medical costs of lung cancer caused by PAHs exposure decreased by 46.1% around the

505 BS region and by an even greater 54.5% at TJ. This illustrated that the implementation of air pol-
506 lution control not only reduced the risk of lung cancer caused by PAHs exposure around the BS
507 region, but also created significant health benefit in the direct medical costs of lung cancer, espe-
508 cially in tightly controlled areas such as TJ. Therefore, the above results noted that more precise
509 pollution prevention and control could better reduce the emission of the pollutants, and sequentially
510 reduce the health risk of human expose.

511

512 **4 Conclusions**

513 A five-year atmospheric PAHs observation was conducted at twelve sites around the BS from
514 June 2014 to May 2019. The five-year atmospheric concentration of Σ_{15} PAHs was 56.78 ± 4.75 ng
515 m^{-3} , characterized by dominant LMW-PAHs ($58.7 \pm 7.8\%$). The maximum annual concentrations
516 and seasonal concentrations occurred in the first year and every winter, respectively. The concen-
517 trations of Σ_{15} PAHs in the atmosphere reduced significantly around the BS, especially at the sam-
518 pling site of TJ during the sampling period. The contributions of coal combustion and vehicle emis-
519 sion to PAHs in the atmosphere during the sampling period showed an increase and a decrease
520 around the BS, respectively. However, the variations of coal combustion and vehicle emission in
521 the source contributions in TJ were just the opposite. From 2014 to 2018, the additional lung cancer
522 incidence of lung cancer caused by PAH exposure around the BS dropped by 74.1%, and a higher
523 drop of 91.6% in TJ. From the statistical standpoint, the drop of the incidence saved about \$10.7
524 million for the total direct medical costs of lung cancer caused by PAHs exposure around the BS.
525 Compared to without air pollution control, the total direct medical costs of lung cancer caused by
526 PAHs exposure decreased by 46.1% around the BS region and by an even greater 54.5% at TJ. And
527 it was further be certified that pollution reduction was beneficial to human health. In the fight
528 against air pollution, more precise pollution prevention and control strategies were needed.

529

530 **Data availability.** Corresponding data for the samples can be accessed on request to the corre-
531 sponding author (Chongguo Tian, cgtian@yic.ac.cn)

532

533 **Author contributions.** CT and ZZ designed the research; WM, RS, XW, ZZ, ZS, and CT con-
534 ducted the sample collection; WM, RS, and XW performed the chemical analyses; WM, RS, XW,
535 and CT analyzed the data, carried out the simulations and wrote the original article; ZS, SZ, JT, SC,
536 JL, and GZ helped with article submissions. All authors have given approval to the final version of
537 the manuscript.

538

539 **Competing interests.** The contact author has declared that none of the authors has any competing
540 interests.

541

542 **Acknowledgements.** This study was supported by the National Natural Science Foundation of
543 China - Shandong Joint Fund (U1906215) and the National Natural Science Foundation of China
544 (No. 41977190 and 42177089).

545

546 **Reference**

547 Agudelo-Castañeda, D.M., Teixeira, E.C., Schneider, I.L., Lara, S.R., Silva, L.F.O.: Exposure to
548 polycyclic aromatic hydrocarbons in atmospheric PM_{1.0} of urban environments: Carcinogenic and
549 mutagenic respiratory health risk by age groups, *Environ. Pollut.*, 224, 158-170,
550 <https://doi.org/10.1016/j.envpol.2017.01.075>, 2017.

551 Air quality historical data query.: <https://www.aqistudy.cn/historydata/>, last access: 31 August 2023,
552 [2014-2019](https://doi.org/10.1016/j.scitotenv.2017.03.256).

553 Alves, C.A., Vicente, A.M., Custodio, D., Cerqueira, M., Nunes, T., Pio, C., Lucarelli, F., Calzolari,
554 G., Nava, S., Diapouli, E., Eleftheriadis, K., Querol, X., and Musa Bandowe, B.A.: Polycyclic
555 aromatic hydrocarbons and their derivatives (nitro-PAHs, oxygenated PAHs, and azaarenes) in
556 PM_{2.5} from Southern European cities, *Sci. Total. Environ.*, 595, 494–504,
557 <https://doi.org/10.1016/j.scitotenv.2017.03.256>, 2017.

558 Biache, C., Mansuy-Huault, L., and Faure, P.: Impact of oxidation and biodegradation on the most
559 commonly used polycyclic aromatic hydrocarbon (PAH) diagnostic ratios: Implications for the
560 source identifications, *J. Hazard. Mater.*, 267, 31–39, [https://doi.org/10.1016/j.jhaz-](https://doi.org/10.1016/j.jhazmat.2013.12.036)
561 [mat.2013.12.036](https://doi.org/10.1016/j.jhazmat.2013.12.036), 2014.

562 Bulletin of the State of China's ecological Environment.:
563 <http://www.mee.gov.cn/hjzl/sthjzk/zghjzkgb/>, last access: 31 August 2023, 2021.

564 Cao, M., Wang, M., and Song, F.: Secular trend of lung cancer incidence in Hexi District, Tianjin,
565 1992 – 2012, *Tumor.*, 36, 1330–1334, <https://doi.org/10.3781/j.issn.1000-7431.2016.22.553>, 2016.

566 Chao, S.H., Liu, J.W., Chen, Y.J., Cao, H.B., and Zhang, A.C.: Implications of seasonal control of
567 PM_{2.5}-bound PAHs: An integrated approach for source apportionment, source region identification
568 and health risk assessment, *Environ. Pollut.*, 247, 685–695, [https://doi.org/10.1016/j.en-](https://doi.org/10.1016/j.envpol.2018.12.074)
569 [vpol.2018.12.074](https://doi.org/10.1016/j.envpol.2018.12.074), 2019.

570 Chen, C., Fang, J.L., Shi, W.Y., Li, T.T., and Shi, X.M.: Clean air actions and health plans in China,
571 *Chinese Medical Journal.*, 133, 1609–1611, <https://doi.org/10.1097/cm9.0000000000000888>,
572 2020.

573 Colvin, K.A., Lewis, C., and Galloway, T.S.: Current issues confounding the rapid toxicological
574 assessment of oil spills, *Chemosphere.*, 245, 125585, [https://doi.org/10.1016/j.chemo-](https://doi.org/10.1016/j.chemosphere.2019.125585)
575 [sphere.2019.125585](https://doi.org/10.1016/j.chemosphere.2019.125585), 2020.

576 Ding, Y.H., and Chan, J.C.L.: The East Asian summer monsoon: an overview, *Meteorol. Atmos.*
577 *Phys.*, 89, 117–142, <https://doi.org/10.1007/s00703-005-0125-z>, 2005.

578 Eng, A., Harner, T., and Pozo, K.: A prototype passive air sampler for measuring dry deposition of
579 polycyclic aromatic hydrocarbons, *Environ. Sci. Technol. Let.*, 1, 77–81,
580 <https://doi.org/10.1021/ez400044z>, 2014.

581 Fan, L.P., Fu, S., Wang, X., Fu, Q.Y., Jia, H.H., Xu, H., Qin, G.M., Hu, X., and Cheng, J.P.: Spati-
582 otemporal variations of ambient air pollutants and meteorological influences over typical urban
583 agglomerations in China during the COVID-19 lockdown, *J. ENVIRON. SCI.*, 106, 26–38,
584 <https://doi.org/10.1016/j.jes.2021.01.006>, 2021.

585 Fang, D., Wang, Q., Li, H., Yu, Y., Lu, Y., and Qian, X.: Mortality effects assessment of ambient
586 PM_{2.5} pollution in the 74 leading cities of China, *Sci. Total. Environ.*, 569-570, 1545–1552,
587 <https://doi.org/10.1016/j.scitotenv.2016.06.248>, 2016.

588 Fang, Y., Chen, Y., Tian, C., Lin, T., Hu, L., Li, J., Zhang, G.: Application of PMF receptor model
589 merging with PAHs signatures for source apportionment of black carbon in the continental shelf
590 surface sediments of the Bohai and Yellow Seas, China, *J. Geophys. Res-Oceans.*, 121, 1346–1359,
591 <https://doi.org/10.1002/2015JC011214>, 2016.

592 Feng, J., Guo, Z., Chan, C.K., and Fang, M.: Properties of organic matter in PM_{2.5} at Changdao
593 Island, China - A rural site in the transport path of the Asian continental outflow, *Atmos. Environ.*,
594 41, 1924–1935, <https://doi.org/10.1016/j.atmosenv.2006.10.064>, 2007.

595 Gao, Y., Guo, X., Ji, H., Li, C., Ding, H., Briki, M., Tang, L., and Zhang, Y.: Potential threat of
596 heavy metals and PAHs in PM_{2.5} in different urban functional areas of Beijing, *Atmos. Res.*, 178-
597 179, 6–16, <https://doi.org/10.1016/j.atmosres.2016.03.015>, 2016.

598 Gibbs, G.W.: Estimating residential polycyclic aromatic hydrocarbon (PAH) related lung cancer
599 risks using occupational data, *The Annals of Occupational Hygiene.*, 41, 49–53,
600 https://doi.org/10.1093/ANNHYG/41.INHALED_PARTICLES_VIII.49, 1997.

601 Gong, P., Wang, X.P., and Yao, T.D.: Ambient distribution of particulate- and gas-phase n-alkanes
602 and polycyclic aromatic hydrocarbons in the Tibetan Plateau, *Environ. Earth. Sci.*, 64, 1703–1711,
603 <https://doi.org/10.1007/s12665-011-0974-3>, 2011.

604 Guo, X., Zhao, L., Chen, D., Jia, Y., Zhao, N., Liu, W., and Cheng, S.: Air quality improvement
605 and health benefit of PM_{2.5} reduction from the coal cap policy in the Beijing-Tianjin-Hebei (BTH)
606 region, China, *Environ. Sci. Pollut. R.*, 25, 32709–32720, [https://doi.org/10.1007/s11356-018-](https://doi.org/10.1007/s11356-018-3014-y)
607 [3014-y](https://doi.org/10.1007/s11356-018-3014-y), 2018.

608 Han, M., Liu, S., Liu, M., Lu, M., Yan, W., He, Y., Dang, H., Dai, X., Zhang, Z., Du, X., and Meng,
609 F.: Assessment of the effect of the reduction of the residential coal combustion on the atmospheric
610 BaP pollution in Beijing-Tianjin-Hebei region, China *Environmental Science.*, 38, 3262–3272,
611 <https://doi.org/10.19674/j.cnki.issn1000-6923.2018.0350-en>, 2018.

612 Hong, W.J., Jia, H., Ma, W.L., Sinha, R.K., Moon, H.B., Nakata, H., Nguyen Hung, M., Chi, K.H.,
613 Li, W.L., Kannan, K., Sverko, E., and Li, Y.F.: Distribution, fate, inhalation exposure and lung
614 cancer risk of atmospheric polycyclic aromatic hydrocarbons in some Asian countries, *Environ.*
615 *Sci. Technol.*, 50, 7163–7174, <https://doi.org/10.1021/acs.est.6b01090>, 2016.

616 Huang, C., Wang, Q., Wang, S., Ren, M., Ma, R., and He, Y.: Air pollution prevention and control
617 policy in China, *Adv. Exp. Med. Biol.*, 1017, 243–261, [https://doi.org/10.1007/978-981-10-5657-](https://doi.org/10.1007/978-981-10-5657-4_11)
618 [4_11](https://doi.org/10.1007/978-981-10-5657-4_11), 2017.

619 Huang, H.Y., Shi, J.F., Guo, L.W., Zhu, X.Y., Wang, L., Liao, X.Z., Liu, G.X., Bai, Y.N., Mao, A.Y.,
620 Ren, J.S., Sun, X.J., Zhang, K., He, J., Dai, M.: Expenditure and financial burden for common
621 cancers in China: a hospital-based multicentre cross-sectional study, *Lancet.*, 388, 10–10,
622 [https://doi.org/10.1016/S0140-6736\(16\)31937-7](https://doi.org/10.1016/S0140-6736(16)31937-7), 2016.

623 Jaward, T.M., Zhang, G., Nam, J.J., Sweetman, A.J., Obbard, J.P., Kobara, Y., and Jones, K.C.:
624 Passive air sampling of polychlorinated biphenyls, organochlorine compounds, and polybromin-
625 ated diphenyl ethers across Asia, *Environ. Sci. Technol.*, 39, 8638–8645,
626 <https://doi.org/10.1021/es051382h>, 2005.

627 Křůmal, K., Mikuška, P.: Mass concentrations and lung cancer risk assessment of PAHs bound to
628 PM1 aerosol in six industrial, urban, and rural areas in the Czech Republic, Central Europe, *Atmos.*
629 *Pollut. Res.*, 11, 401-408, <https://doi.org/10.1016/j.apr.2019.11.012>, 2020.

630 Li, N., Zhang, X., Shi, M., and Hewings, G.J.D.: Does China's air pollution abatement policy matter?
631 An assessment of the Beijing-Tianjin-Hebei region based on a multi-regional CGE model, *Energ.*
632 *Policy.*, 127, 213–227, <https://doi.org/10.1016/j.enpol.2018.12.019>, 2019.

633 Li, W., Park, R., Alexandrou, N., Dryfhout-Clark, H., Brice, K., and Hung, H.: Multi-year analyses
634 reveal different trends, sources, and implications for source-related human health risks of atmos-
635 pheric polycyclic aromatic hydrocarbons in the Canadian Great Lakes Basin, *Environ. Sci. Tech-*
636 *no.*, 55, 2254–2264, <https://doi.org/10.1021/acs.est.0c07079>, 2021.

637 Li, Z.Y., Wang, Y.T., Li, Z.X., Guo, S.T., and Hu, Y.: Levels and Sources of PM_{2.5}-associated PAHs
638 during and after the Wheat Harvest in a Central Rural Area of the Beijing-Tianjin-Hebei (BTH)
639 Region, *Aerosol. Air. Qual. Res.*, 20, 1070–1082, <https://doi.org/10.4209/aaqr.2020.03.0083>, 2020.
640 Lian, L., Huang, T., Ling, Z., Li, S., Li, J., Jiang, W., Gao, H., Tao, S., Liu, J., Xie, Z., Mao, X.,
641 Ma, J.: Interprovincial trade driven relocation of polycyclic aromatic hydrocarbons and lung cancer
642 risk in China, *J. Clean. Prod.*, 280, 124368, <https://doi.org/10.1016/j.jclepro.2020.124368>, 2021.
643 Liang, X., Tian, C., Zong, Z., Wang, X., Jiang, W., Chen, Y., Ma, J., Luo, Y., Li, J., Zhang, G.: Flux
644 and source-sink relationship of heavy metals and arsenic in the Bohai Sea, China, *Environ. Pollut.*,
645 242, 1353-1361, <https://doi.org/10.1016/j.envpol.2018.08.011>, 2018.
646 Liao, C.M., Chio, C.P., Chen, W.Y., Ju, Y.R., Li, W.H., Cheng, Y.H., Liao, V.H.C., Chen, S.C., Ling,
647 M.P.: Lung cancer risk in relation to traffic-related nano/ultrafine particle-bound PAHs exposure:
648 A preliminary probabilistic assessment, *J. Hazard. Mater.*, 190, 150-158,
649 <https://doi.org/10.1016/j.jhazmat.2011.03.017>, 2011.
650 Lin, Y., Ma, Y., Qiu, X., Li, R., Fang, Y., Wang, J., Zhu, Y., and Hu, D.: Sources, transformation,
651 and health implications of PAHs and their nitrated, hydroxylated, and oxygenated derivatives in
652 PM_{2.5} in Beijing, *Journal of Geophysical Research.*, 120, 7219–7228,
653 <https://doi.org/10.1002/2015JD023628>, 2015.
654 Liu, H., Li, B., Qi, H., Ma, L., Xu, J., Wang, M., Ma, W., and Tian, C.: Source apportionment and
655 toxic potency of polycyclic aromatic hydrocarbons (PAHs) in the air of Harbin, a cold city in North-
656 ern China, *Atmosphere-Basel.*, 12, <https://doi.org/10.3390/atmos12030297>, 2021.
657 Liu, W.J., Xu, Y.S., Zhao, Y.Z., Liu, Q.Y., Yu, S.Y., Liu, Y., Wang, X., Liu, Y., Tao, S., and Liu,
658 W.X.: Occurrence, source, and risk assessment of atmospheric parent polycyclic aromatic hydro-
659 carbons in the coastal cities of the Bohai and Yellow Seas, China, *Environ. Pollut.*, 254,
660 <https://doi.org/10.1016/j.envpol.2019.113046>, 2019.
661 Luo, M., Ji, Y.Y., Ren, Y.Q., Gao, F.H., Zhang, H., Zhang, L.H., Yu, Y.Q., and Li, H.: Characteristics
662 and health risk assessment of PM_{2.5}-bound PAHs during heavy air pollution episodes in winter in
663 urban area of Beijing, China, *Atmosphere-Basel.*, 12, 323, <https://doi.org/10.3390/atmos12030323>,

664 2021.

665 Lv, Min., Luan, Xiaolin., Liao, Chunyang., Wang, Dongqi., Liu, Dongyan., Zhang, Gan., Jiang,
666 Guibin., Chen, Lingxin.: Human impacts on polycyclic aromatic hydrocarbon distribution in Chi-
667 nese intertidal zones, *Nature. Sustainability.*, <https://doi.org/10.1038/s41893-020-0565-y>, 2020.

668 Ma, W.L., Li, Y.F., Qi, H., Sun, D.Z., Liu, L.Y., and Wang, D.G.: Seasonal variations of sources of
669 polycyclic aromatic hydrocarbons (PAHs) to a northeastern urban city, China, *Chemosphere.*, 79,
670 441–447, <https://doi.org/10.1016/j.chemosphere.2010.01.048>, 2010.

671 Ma, W.L., Liu, L.Y., Jia, H.L., Yang, M., and Li, Y.F.: PAHs in Chinese atmosphere Part I: Concen-
672 tration, source and temperature dependence, *Atmos. Environ.*, 173, 330–337,
673 <https://doi.org/10.1016/j.atmosenv.2017.11.029>, 2018.

674 Ma, W.L., Zhu, F.J., Liu, L.Y., Jia, H.L., Yang, M., and Li, Y.F.: PAHs in Chinese atmosphere Part
675 II: Health risk assessment, *Ecotox. Environ. Safe.*, 200, 110774,
676 <https://doi.org/10.1016/j.ecoenv.2020.110774>, 2020.

677 Ma, Y.X., Xie, Z.Y., Yang, H.Z., Moller, A., Halsall, C., Cai, M.H., Sturm, R., and Ebinghaus, R.:
678 Deposition of polycyclic aromatic hydrocarbons in the North Pacific and the Arctic, *J. Geophys.*
679 *Res-Atmos.*, 118, 5822–5829, <https://doi.org/10.1002/jgrd.50473>, 2013.

680 Marvin, C.H., Tomy, G.T., Thomas, P.J., Holloway, A.C., Sandau, C.D., Idowu, I., and Xia, Z.:
681 Considerations for prioritization of polycyclic aromatic compounds as environmental contaminants,
682 *Environ. Sci. Technol.*, 54, 14787–14789, <https://doi.org/10.1021/acs.est.0c04892>, 2020.

683 Menzler, S., Piller, G., Gruson, M., Rosario, A.S., Wichmann, H.E., and Kreienbrock, L.: Popula-
684 tion attributable fraction for lung cancer due to residential radon in Switzerland and Germany,
685 *Health. Phys.*, 95, 179–189, <https://doi.org/10.1097/01.Hp.0000309769.55126.03>, 2008.

686 Moeckel, C., Harner, T., Nizzetto, L., Strandberg, B., Lindroth, A., and Jones, K.C.: Use of depu-
687 ration compounds in passive air samplers: results from active sampling-supported field deployment,
688 potential uses, and recommendations, *Environ. Sci. Technol.*, 43, 3227–3232,
689 <https://doi.org/10.1021/es802897x>, 2009.

690 Paatero, P., Eberly, S., Brown, S.G., and Norris, G.A.: Methods for estimating uncertainty in factor
691 analytic solutions, *Atmos. Meas. Tech.*, 7, 781–797, <https://doi.org/10.5194/amt-7-781-2014>, 2014.

692 Qu, L., Yang, L., Zhang, Y., Wang, X., Sun, R., Li, B., Lv, X., Chen, Y., Wang, Q., Tian, C., and Ji,
693 L.: Source Apportionment and Toxic Potency of PM_{2.5}-Bound Polycyclic Aromatic Hydrocarbons
694 (PAHs) at an Island in the Middle of Bohai Sea, China, *Atmosphere.*, 13, [https://doi.org/10.3390/at-](https://doi.org/10.3390/atmos13050699)
695 [mos13050699](https://doi.org/10.3390/atmos13050699), 2022.

696 Ramírez, N., Cuadras, A., Rovira, E., Marcé, R.M., Borrull, F.: Risk Assessment Related to Atmos-
697 pheric Polycyclic Aromatic Hydrocarbons in Gas and Particle Phases near Industrial Sites, *Environ.*
698 *Health. Perspect.*, 119, 1110-1116, <https://doi.org/10.1289/ehp.1002855>, 2011.

699 Shi, C.L., Lou, P.A., Shi, J.F., Huang, H.Y., Li, J., Yue, Y.P., Wang, L., Dong, Z.M., Chen, P.P.,
700 Zhang, P., Zhao, C.Y., Li, F., Zhou, J.Y., and Dai, M.: Economic burden of lung cancer in mainland
701 China, 1996-2014: a systematic review, *China Journal of Public Health.*, 33, 1767–1774,
702 <https://doi.org/10.11847/zgggws2017-33-12-25>, 2017.

703 Sofowote, U.M., Hung, H., Rastogi, A.K., Westgate, J.N., Deluca, P.F., Su, Y.S., and McCarry, B.E.:
704 Assessing the long-range transport of PAH to a sub-Arctic site using positive matrix factorization
705 and potential source contribution function, *Atmos. Environ.*, 45, 967–976,
706 <https://doi.org/10.1016/j.atmosenv.2010.11.005>, 2011.

707 Sun, R., Wang, X., Tian, C., Zong, Z., Ma, W., Zhao, S., Wang, Y., Tang, J., Cui, S., Li, J., and
708 Zhang, G.: Exploring source footprint of Organophosphate esters in the Bohai Sea, China: Insight
709 from temporal and spatial variabilities in the atmosphere from June 2014 to May 2019, *Environ.*
710 *Int.*, 159, <https://doi.org/10.1016/j.envint.2021.107044>, 2022.

711 Sun, Z., Zong, Z., Tian, C., Li, J., Sun, R., Ma, W., Li, T., Zhang, G.: Reapportioning the sources
712 of secondary components of PM_{2.5}: combined application of positive matrix factorization and iso-
713 topic evidence, *Sci. Total. Environ.*, 764, <https://doi.org/10.1016/j.scitotenv.2020.142925>, 2021.

714 Taghvaei, S., Sowlat, M.H., Hassanvand, M.S., Yunesian, M., Naddafi, K., Sioutas, C.: Source-
715 specific lung cancer risk assessment of ambient PM_{2.5}-bound polycyclic aromatic hydrocarbons

716 (PAHs) in central Tehran, *Environ. Int.*, 120, 321-332, <https://doi.org/10.1016/j.envint.2018.08.003>,
717 2018.

718 Tan, J.H., Bi, X.H., Duan, J.C., Rahn, Kenneth A., Sheng, G.Y., and Fu, J.M.: Seasonal variation
719 of particulate polycyclic aromatic hydrocarbons associated with PM₁₀ in Guangzhou, China, *Atmos.*
720 *Res.*, 80, 250–262, <https://doi.org/10.1016/j.atmosres.2005.09.004>, 2006.

721 Tian, C., Ma, J., Liu, L., Jia, H., Xu, D., and Li, Y.F.: A modeling assessment of association between
722 East Asian summer monsoon and fate/outflow of α -HCH in Northeast Asia, *Atmos. Environ.*, 43,
723 3891-3901, <https://doi.org/https://doi.org/10.1016/j.atmosenv.2009.04.056>, 2009.

724 Tong, L., Peng, C.H., Huang, Z.W., Zhang, J.J., Dai, X.R., Xiao, H., Xu, N.B., and He, J.: Identifying the pollution characteristics of atmospheric polycyclic aromatic hydrocarbons associated
725 with functional districts in Ningbo, China, *B. Environ. Contam. Tox.*, 103, 34–40,
726 <https://doi.org/10.1007/s00128-018-02535-4>, 2019.

727 Wang, X.P., Zong, Z., Tian, C.G., Chen, Y.J., Luo, C.L., Tang, J.H., Li, J., Zhang, G.: Assessing on
728 toxic potency of PM_{2.5}-bound polycyclic aromatic hydrocarbons at a national atmospheric back-
729 ground site in North China, *Sci. Total. Environ.*, 612, 330–338, <https://doi.org/10.1016/j.scitotenv.2017.08.208>, 2018.

730 Wu, D., Xu, Y., and Zhang, S.: Will joint regional air pollution control be more cost-effective? An
731 empirical study of China's Beijing-Tianjin-Hebei region, *J. Environ. Manage.*, 149, 27–36,
732 <https://doi.org/10.1016/j.jenvman.2014.09.032>, 2015.

733 Xing, X., Chen, Z., Tian, Q., Mao, Y., Liu, W., Shi, M., Cheng, C., Hu, T., Zhu, G., Li, Y., Zheng,
734 H., Zhang, J., Kong, S., and Qi, S.: Characterization and source identification of PM_{2.5}-bound pol-
735 ycyclic aromatic hydrocarbons in urban, suburban, and rural ambient air, central China during sum-
736 mer harvest, *Ecotox. Environ. Safe.*, 191, <https://doi.org/10.1016/j.ecoenv.2020.110219>, 2020.

737 Yan, Z., Jin, L., Chen, X., Wang, H., Tang, Q., Wang, L., and Lei, Y.: Assessment of air pollutants
738 emission reduction potential and health benefits for residential heating coal changing to electricity
739 in the Beijing-Tianjin-Hebei region, *Research of Environmental Sciences.*, 32, 95–103,
740 <https://doi.org/10.13198/j.issn.1001-6929.2018.10.16>, 2019.

743 Yang, Q.Q., Yuan, Q.Q., Li, T.W., Shen, H.F., and Zhang, L.P.: The relationships between PM_{2.5}
744 and meteorological factors in China: seasonal and regional variations, *Int. J. Env. Res. Pub. He.*,
745 14, <https://doi.org/10.3390/ijerph14121510>, 2017.

746 Yu, Q.Q., Gao, B., Li, G.H., Zhang, Y.L., He, Q.F., Deng, W., Huang, Z.H., Ding, X., Hu, Q.H.,
747 Huang, Z.Z., Wang, Y.J., Bi, X.H., and Wang, X.M.: Attributing risk burden of PM_{2.5}-bound poly-
748 cyclic aromatic hydrocarbons to major emission sources: Case study in Guangzhou, south China,
749 *Atmos. Environ.*, 142, 313–323, <https://doi.org/10.1016/j.atmosenv.2016.08.009>, 2016.

750 Zhang, J., Liu, W., Xu, Y., Cai, C., Liu, Y., Tao, S., and Liu, W.: Distribution characteristics of and
751 personal exposure with polycyclic aromatic hydrocarbons and particulate matter in indoor and out-
752 door air of rural households in Northern China, *Environ. Pollut.*, 255, 113176,
753 <https://doi.org/10.1016/j.envpol.2019.113176>, 2019.

754 Zhang, J.W., Feng, L.H., Zhao, Y., Hou, C.C., and Gu, Q.: Health risks of PM_{2.5}-bound polycyclic
755 aromatic hydrocarbon (PAH) and heavy metals (PPAH&HM) during the replacement of central
756 heating with urban natural gas in Tianjin, China, *Environ. Geochem. Hlth.*, 44, 2495–2514,
757 <https://doi.org/10.1007/s10653-021-01040-8>, 2021.

758 Zhang, J.W., Zhao, J., Cai, J., Gao, S.T., Li, J., Zeng, X.Y., and Yu, Z.Q.: Spatial distribution and
759 source apportionment of atmospheric polycyclic aromatic hydrocarbons in the Pearl River Delta,
760 China, *Atmos. Pollut. Res.*, 9, 887–893, <https://doi.org/10.1016/j.apr.2018.02.004>, 2018.

761 Zhang, S.W., Chen, W.Q., Kong, L.Z., Li, G.L., and Zhao, P.: An Annual Report: Cancer Incidence
762 in 35 Cancer Registries in China, 2003, *China Cancer.*, 494–507,
763 <https://doi.org/10.3969/j.issn.1004-0242.2007.07.001>, 2007.

764 Zhang, X., Leng, S., Qiu, M., Ding, Y., Zhao, L., Ma, N., Sun, Y., Zheng, Z., Wang, S., Li, Y., Guo,
765 X.: Chemical fingerprints and implicated cancer risks of Polycyclic aromatic hydrocarbons (PAHs)
766 from fine particulate matter deposited in human lungs, *Environ. Int.*, 173,
767 <https://doi.org/10.1016/j.envint.2023.107845>, 2023.

768 Zhang, Y.J., Lin, Y., Cai, J., Liu, Y., Hong, L.N., Qin, M.M., Zhao, Y.F., Ma, J., Wang, X.S., Zhu,
769 T., Qiu, X.H., and Zheng, M.: Atmospheric PAHs in North China: Spatial distribution and sources,
770 *Sci. Total. Environ.*, 565, 994–1000, <https://doi.org/10.1016/j.scitotenv.2016.05.104>, 2016.

771 Zhang, Y.X., Tao, S., Cao, J., and Coveney, R.M.: Emission of polycyclic aromatic hydrocarbons
772 in China by county, *Environ. Sci. Technol.*, 41, 683–687, <https://doi.org/10.1021/es061545h>, 2007.

773 Zhang, Y.X., Tao, S., Shen, H.Z., and Ma, J.M.: Inhalation exposure to ambient polycyclic aromatic
774 hydrocarbons and lung cancer risk of Chinese population, *P. Natl. Acad. Sci. USA.*, 106,
775 21063–21067, <https://doi.org/10.1073/pnas.0905756106>, 2009.

776 Zhao, H., Wu, R., Liu, Y., Cheng, J., Geng, G., Zheng, Y., Tian, H., He, K., and Zhang, Q.: Air
777 pollution health burden embodied in China's supply chains, *Environmental Science and Ecotech-*
778 *nology.*, 16, 100264–100264, <https://doi.org/10.1016/j.es.2023.100264>, 2023.

779 Zhi, Z., Wang, W., Cheng, M., Liu, S., Xu, J., He, Y., and Meng, F.: The contribution of residential
780 coal combustion to PM_{2.5} pollution over China's Beijing-Tianjin-Hebei region in winter, *Atmos.*
781 *Environ.*, 159, 147–161, <https://doi.org/10.1016/j.atmosenv.2017.03.054>, 2017.

782 Zhu, D., Tao, S., Wang, R., Shen, H., Huang, Y., Shen, G., Wang, B., Li, W., Zhang, Y., Chen, H.,
783 Chen, Y., Liu, J., Li, B., Wang, X., Liu, W.: Temporal and spatial trends of residential energy con-
784 sumption and air pollutant emissions in China. *Applied Energy* 106, 17-24,
785 <https://doi.org/10.1016/j.apenergy.2013.01.040>, 2013.

786 Zhuo, S., Shen, G., Zhu, Y., Du, W., Pan, X., Li, T., Han, Y., Li, B., Liu, J., Cheng, H., Xing, B.,
787 and Tao, S.: Source-oriented risk assessment of inhalation exposure to ambient polycyclic aromatic
788 hydrocarbons and contributions of non-priority isomers in urban Nanjing, a megacity located in
789 Yangtze River Delta, China, *Environ. Pollut.*, 224, 796–809, <https://doi.org/10.1016/j.en->
790 [vpol.2017.01.039](https://doi.org/10.1016/j.environpol.2017.01.039), 2017.